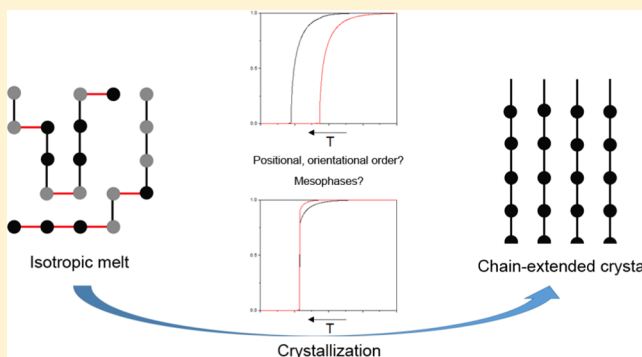


Study on the Thermodynamics of Polymer Crystallization Based on Twin-Lattice Model

Nuofei Jiang, Ping Tang,* Hongdong Zhang, and Yuliang Yang*

State Key Laboratory of Molecular Engineering of Polymers, Department of Macromolecular Science, Fudan University, Shanghai 200433, China

ABSTRACT: Polymer crystallization is the most important part in determining the performance of polymeric materials. The twin-lattice model originally provided by Lennard-Jones and Devonshire, developed by Pople and Karasz and other researchers, is extended for describing the thermodynamics of polymer crystallization. The positional order of segments and the orientational order of bonds are considered in this model. The free energy of polymers is obtained by further introducing the conformational energy and entropy, and thus a new parameter is defined, which is the ratio of conformational energy and positional diffusion energy. We studied two kinds of processes in polymer crystallization, including the process with plastic crystal phase and without any mesophases. The choice of crystallizing process is determined by the magnitude of lattice energy and conformational energy. The solid–solid transition from crystal to plastic crystal shows a significant dependence on the conformational energy. Considering data reliability, *n*-paraffins are chosen as the representation of polymers to compare the predictions of the model with experimental observations. We predict the number of carbons beyond which the rotator phase disappears, which is quite in agreement with the experiments. These calculations and results show this model can provide a new understanding to the crystallization of polymers.



INTRODUCTION

The performance of polymeric materials primarily depends on their physical states. Therefore, the crystallization of polymers plays an important role not only in the scientific understanding of condensed matter but also in their pervasive applications and technological development. A great variety of phases are found during the process of crystallization or melting, according to the molecular structure as well as molecular motion.^{1,2} Although some of these phases belong to non-equilibrium or metastable states, they are defined in a thermodynamic way. As has been widely recognized, each transition between these states is related to the appearance or disappearance of some kind of symmetry.³ In a mean-field point of view, these symmetries are represented by positional and orientational ordering. Therefore, the key issue in a polymer crystallization theory is how to build these two kinds of ordering on the basis of a theoretical model.

Positional or translational ordering–disordering is proposed to differentiate isotropic small molecules in the solid and liquid phases. For example, in inert gases, positional ordering–disordering is accurately enough to describe the liquid-to-crystal transition behavior. The position of a molecule is fixed in the solid, whereas migration between two positions is allowed in the liquid. This leads to different properties of the solid and liquid. In phenomenological researches, it is a common treatment to translate the difference between solids and liquids into a nonconserved order parameter.^{4–7} Mean-

while, many other attempts have been made in explaining the melting nature from a molecular point of view.^{8–10} Of these theories, what interests us most is the so-called twin-lattice model proposed by Lennard-Jones and Devonshire.⁴ In this model, it is assumed that the physical state of molecules could be pictured as the mixture of molecules and structureless “holes” in a hypothetical lattice. Each lattice has two sites to accommodate all molecules and holes. This is analogous to the overlying of two interpenetrated sets of lattices, and thus we rename it as the twin-lattice model, referred to as α and β lattices. When molecules tend to occupy one kind of lattice, say α or β sites, the motion of each molecule is confined, thus becoming positional ordered, corresponding to the solid state. When molecules distribute randomly in the two kinds of lattices, the positions of molecules are not confined, namely, positional disordered, and thus can be identified as the liquid state. If the energy for a molecule to diffuse from a mainly α lattice to the interstitial β sites zW is defined, where z is the number of β sites closest to any one α site, the phase transition between the two states can be calculated. It is clear the key issue of this method is the allowance for the possibility of molecular positional disorder, by taking advantage of the twin-lattice model.

Received: June 23, 2018

Revised: August 16, 2018

Published: August 16, 2018

However, orientational ordering–disordering is an additional specific feature in a geometrically anisotropic molecule system. Its coupling with positional ordering–disordering results in the appearance of mesophases like plastic crystal and liquid crystal. Several theories have been successful in explaining the orientation-related transitions, such as the Maier–Saupe theory¹¹ and Landau–de Gennes theory¹² for describing nematic–isotropic transition in thermotropic liquid crystals. The twin-lattice model was also developed for considering the anisotropies of small molecules, and Pople and Karasz made the first attempt.^{13,14} In their modified model, two orientations are allowed for each molecule so the molecules will have four optional states (two kinds of lattice sites and two orientations for each site). They further introduce the energy barrier $z'W'$ for molecular rotation, when all neighboring molecules are in the same kind of lattice site and arranged in the same orientation, where z' is the coordinate number of the α -lattice (or β -lattice) itself. The relative energy barrier describing the competition for the molecular rotation and positional diffusion, $v_{PK} = z'W'/zW$, becomes the key parameter. The value of v_{PK} determines the phase transition behaviors evaluated from this theory, which agrees well with some experiments. For example, in the differential thermal analysis of cycloalkanes under high pressure, the small volume change of the solid II-to-solid III transition is consistent with the Pople–Karasz model calculations.¹⁵ The proton magnetic resonance results of the XMe_4 family molecules, where $X = C, Si, \text{ and } Ge$, show that these molecules can be assigned with an accurate number of v_{PK} and agree with the qualitative features of the Pople–Karasz model as well.¹⁶ On the basis of Pople and Karasz, further modification is applied to the twin-lattice model.^{17–25} In contrast to two orientations in Pople and Karasz model, Amzel and Becka¹⁷ allow the number of orientations as a new parameter, which can be obtained from the molecular point group symmetry or the measured solid–solid transition entropy. Chandrasekhar^{18–20} modified the volumetric dependence of the rotational energy barrier W' . Then, the liquid crystal phase is successfully calculated and the theoretical prediction gives a better agreement with experiments. Keskin and Özgan^{21–24} divided the repulsive energy into two parts, so a third energetic parameter is included. A complete picture of phase transition is given on the basis of the modifications. They have also investigated the dynamic behavior of the twin-lattice model by the direct relaxation method and path probability method.²⁵

Because of the long-chain characteristics, it is indispensable to consider both the positional and orientational ordering of polymers in crystallization. The anisotropic interaction is a necessary driving force in this process.²⁶ There are also arguments that some mesophases may be the intermediate states in the formation of polymer spherulites,²⁷ indicating the coupling of the two kinds of ordering plays an important role in the crystallization dynamics. In spite of the advances in experiment, simulation, and theory,^{28–31} the molecular mechanism of polymer crystallization is still not fully understood. As a result, we expect to extend the twin-lattice model to polymer systems in this paper. As far as we know, this is the first attempt to do this extension. Besides, lattice theories have been successful in describing the characters of polymers in multiple scales. For instance, the Flory–Huggins lattice theory^{32,33} has proven to be the most successful thermodynamic theory for polymer blends and solution. In this model,

polymer solutions and blends are coarse-grained but the details in concentration distribution are maintained. To bridge the macroscopic phase state with the microscopic molecular structure, we try to offer this intuitive idea to understand the thermodynamic phase transition behavior in polymer crystallization. Furthermore, theoretical predictions are compared with the experimental data of n -paraffins whose phase transition behaviors are chosen as the representation of polymer crystallization, due to availability of accurate data of their thermodynamic equilibrium state.

TWIN-LATTICE MODEL FOR POLYMER STATISTICAL THERMODYNAMICS

We follow the basic assumptions by Lennard-Jones and Devonshire,⁴ to give a lattice description for polymer crystallization thermodynamics. Identically, we introduce the two interpenetrated α and β lattices to accommodate segments of polymers. The relative location of the two lattices is redrawn, as illustrated in Figure 1, just to prevent a

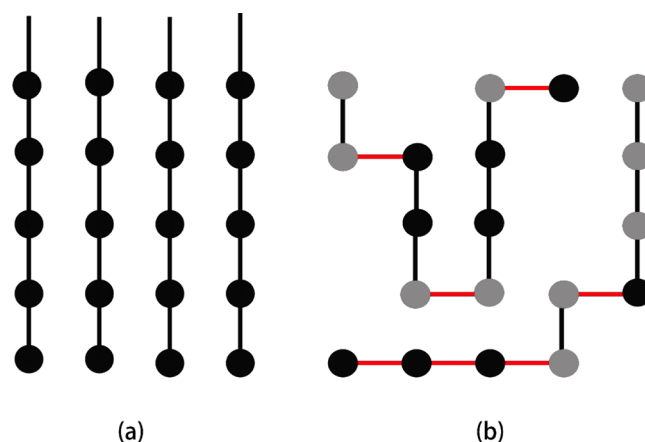


Figure 1. Schematic shown of a twin-lattice model for polymers with each segment having two orientations, namely, $D = 2$. (a) Representing chain-extended polymer crystal. (b) Polymer melt. Black and red lines stand for bonds in different orientations.

misunderstanding after the orientations of polymers are introduced. For a sample composed of N ($N = n_p \times x$, where n_p is the number of chains and x is the chain length) segments, the number of α and β lattice sites are both set as N so there are totally $2N$ lattice sites, leaving N sites for structureless holes, available for describing ordering and disordering. We use φ ($0 \leq \varphi \leq 1$), the fraction of segments in lattice α (or β), as the positional order parameter. Lattice α and β are equal in physics, which means φ and $1 - \varphi$ stand for the same states. In this case, the value of φ is in the range of $0.5 \leq \varphi \leq 1$. It is convenient to normalize the positional order parameter as $\Phi = 2\varphi - 1$, to meet the usual expression. As is generally accepted, $\Phi = 0$ corresponds to the liquid phase of polymers and $\Phi = 1$ corresponds to the solid phase. For simplification, the value of Φ is considered to be equal in every single chain and thus there are $x(1 + \Phi)/2$ α -lattice segments and $x(1 - \Phi)/2$ β -lattice segments in one polymer chain.

In the most primitive model, a polymer chain is described as a set of end-to-end vectors. They are the representation of chain conformation and equal to the chemical bonds inside the chain. When we are talking about the orientation of a flexible polymer chain, all of these vectors should be included to

distinguish ordering and disordering, for a single overall end-to-end vector is not enough completely. So the orientational ordering is closely related to the chain conformation. For this reason, the orientational order parameter is constructed from the chemical bonds inside the chain. We notice that the definition of “bond orientation” has been used to describe some specific ordering like quasicrystalline.³⁴ It should be emphasized that the bond orientation in this paper is just another form of molecular orientation, unlike the quasicrystal-like case. In the present model, it is assumed that total D ($D \geq 2$) orientations are permitted for each bond, as proposed by Amzel and Becka.¹⁷ The orientational order parameter can be defined as the fraction of bonds in one specific orientation to the totally possible orientations, θ ($1/D \leq \theta \leq 1$). Bonds in the rest of the $D - 1$ orientations are thus regarded to have the same fraction $(1 - \theta)/(D - 1)$. Normalization is conducted as well, by defining $\Theta = (D\theta - 1)/(D - 1)$. In this way, $\Theta = 0$ represents the isotropic state where the chains are random coils and $\Theta = 1$ represents the anisotropic state with the rigid rodlike chain conformation.

So far, the basic structure information of polymers in a twin-lattice model is established. The macroscopic state is associated with the microscopic arrangement of segments described by the order parameters. Therefore, all kinds of ordered phases can be described according to positional and orientational order parameters mentioned above. For example, our model can describe various states, including chain-extended crystal ($\Phi = 1, \Theta = 1$), plastic crystal ($\Phi = 1, \Theta = 0$), liquid crystal ($\Phi = 0, \Theta = 1$), disordered melts ($\Phi = 0, \Theta = 0$), and the mesophases or metastable phases that can be observed during the crystallization process. The phase transitions among these states provide the thermodynamic driving force such as for crystallization, which determines the dynamics of polymer crystallization. As a result, we present quantitative analysis to investigate the phase transition behaviors of this model in the following context. To be noted, glassy state will not be included in our discussions. Polymers in the twin-lattice model are considered perfect in structure so that all segments are able to be arranged into the crystalline region. The occurrence of a glassy state is only the result of molecular motions, which is beyond the scope of thermodynamics. In this case, the glassy state is essentially equal to the melt in the molecular structure so its order parameters should be $\Phi = 0$ and $\Theta = 0$.

Free-Energy Calculation. On the basis of the assumption of the twin-lattice model and mean-field treatment, we have the analytical expression of free energy. The contribution of chain connectivity is specified, and the equation should return to the Pople–Karasz expression^{13,14} in a specific case. The most ordered phase, or chain-extended crystal, is set as the reference. So we focus on the difference in symmetries, which plays the most essential role in phase transitions.

The free energy in the twin-lattice system can be treated separately. The entropy change is composed of three parts as follows

$$\Delta S[\Phi, \Theta] = \Delta S_p + \Delta S_o + \Delta S_c \quad (1)$$

where the positional part ΔS_p and the orientational part ΔS_o come from the permutation of segments and bonds, namely, translational entropy, which are consistent with small molecular systems, as described by Pople and Karasz.¹³ They are calculated by adopting the Bragg–Williams approximation³⁵ in the form as

$$\frac{\Delta S_p}{Nk_B} = -(1 + \Phi) \ln\left(\frac{1 + \Phi}{2}\right) - (1 - \Phi) \ln\left(\frac{1 - \Phi}{2}\right) \quad (2)$$

$$\begin{aligned} \frac{\Delta S_o}{Nk_B} = & -\frac{(D - 1)\Theta + 1}{D} \ln \frac{(D - 1)\Theta + 1}{D} \\ & - \frac{(D - 1)(1 - \Theta)}{D} \ln \frac{(1 - \Theta)}{D} \end{aligned} \quad (3)$$

ΔS_c is the conformational entropy, the most specific part in polymers compared with small molecules. This kind of effect is also the cause of entropic elasticity in chain statistics, which is the driving force in the process of melting and crystallizing. The Flory–Huggins theory has shown how to treat the connected segments in a lattice model.³² We thus follow a similar process, and ΔS_c is represented as follows. See the Appendix for derivation details.

$$\frac{\Delta S_c}{Nk_B} = \left(1 - \frac{2}{x}\right) \frac{(D - 1)(1 - \Theta^2)}{D} \ln 2 \quad (4)$$

For calculation convenience, we introduce the so-called “defect” segment, representing a segment whose ends are connecting two different orientational bonds. Its average number is $(x - 2)(D - 1)(1 - \Theta^2)/D$ in each isolated chain. A defect segment is equal to a gauche conformer in real polymeric solids, which exists in deformation structures such as folds and kinks.³⁶ When there are only two segments in a chain, defects effect will disappear and the value of ΔS_c will be zero. As a result, the total entropy ΔS will be the same as that of anisotropic small molecules. The number of conformations of a polymer chain is determined by the orientational distribution of bonds, so it is only a function of Θ . For example, the crystal and liquid crystal phase are both highly orientational ordered and the molecules are both rodlike. They both contain few defect structures and thus have similar conformational entropy.

The enthalpy is composed of three contributions as well

$$\Delta H[\Phi, \Theta] = \Delta H_p + \Delta H_1 + \Delta H_c \quad (5)$$

where the positional part ΔH_p results from the contribution of W_{AB} , the potential between adjacent segments in different lattices. It is the same as the position diffusion energy W in small molecules. Because the interaction is isotropic and not influenced by the connected bond, ΔH_p is expressed as

$$\frac{\Delta H_p}{Nk_B T} = \frac{(1 + \Phi)(1 - \Phi)}{4} \frac{zW_{AB}}{k_B T} \quad (6)$$

ΔH_1 is another part of potential between a pair of segments, which is actually a representation of the lattice energy. This pair of segments is in the same kind of lattice but different in the orientation of connected bonds. In polymers, when there is any deformation structure in the highly crystalline regions, the energy will instantly increase because the neighboring chains remain in a parallel fashion. We use $W_{\alpha\alpha'}$ to represent this kind of energy, which is the same as the rotational energy barrier W' in the Pople–Karasz model. ΔH_1 , related to the defect numbers, is given as follows

$$\frac{\Delta H_1}{Nk_B T} = \frac{(1 + \Phi)^2 + (1 - \Phi)^2}{4} \frac{(D - 1)(1 - \Theta^2)}{2D} \frac{z'W_{\alpha\alpha'}}{k_B T} \quad (7)$$

From eq 7, it is clear ΔH_1 reflects the coupling between positional and orientational ordering. In addition, according to the illustration by McCullough,³⁶ a polymer crystalline environment can be regarded as unconnected crystalline arrays aggregated by relatively low-molecular-weight compounds. So the factor $1 - 2/x$, representing the polymer chain length, should not be included in this formula. This demonstrates the values of $\Delta H_1/N$ are supposed to be constant in different cases of chain length. Hence, ΔH_1 remains nonzero even at $x = 2$, which is consistent with the Pople–Karasz expression for diatomic molecules.

The chain conformation contributes not only additional entropy but also enthalpy, denoted as ΔH_c , especially when polymers are semiflexible. The phase transitions have a strong dependence on the chain rigidity which we shall discuss specifically in the following. In the wormlike chain model^{37,38} for describing semiflexible chain conformation statistics, the conformational energy is proportional to the local curvature. In the current statistic model, we adopt the average energy difference between defect and nondefect segments as

$$\frac{\Delta H_c}{Nk_B T} = \left(1 - \frac{2}{x}\right) \frac{(D-1)(1-\Theta^2)}{D} \frac{W_c}{k_B T} \quad (8)$$

where W_c represents the energy to bend a nondefect segment into a defect one. For the zigzag structure of polyethylene (PE) chains, for example, it represents the energy to transfer a trans conformer to a gauche, estimated to be 500 cal/mol.³⁹

Therefore, the free-energy density of the polymer system is as follows

$$\begin{aligned} \frac{\Delta G}{Nk_B T} = & \frac{(1+\Phi)(1-\Phi)}{4} \frac{zW_{AB}}{k_B T} \\ & + \frac{(1+\Phi)^2 + (1-\Phi)^2}{4} \frac{(D-1)(1-\Theta^2)}{2D} \\ & + \frac{z'W_{\alpha\alpha'}}{k_B T} + (1+\Phi) \ln\left(\frac{1+\Phi}{2}\right) \\ & + (1-\Phi) \ln\left(\frac{1-\Phi}{2}\right) + \frac{(D-1)\Theta + 1}{D} \\ & \ln \frac{(D-1)\Theta + 1}{D} + \frac{(D-1)(1-\Theta)}{D} \\ & \ln \frac{(1-\Theta)}{D} + \left(1 - \frac{2}{x}\right) \frac{(D-1)(1-\Theta^2)}{D} \frac{W_c}{k_B T} \\ & - \left(1 - \frac{2}{x}\right) \frac{(D-1)(1-\Theta^2)}{D} \ln 2 \end{aligned} \quad (9)$$

where the last two terms in the right-hand side show how the chain connectivity influences the relative free energy from the ordered to disordered phase. They are only the functions of Θ and thus have a direct impact on the orientational order. The relative entropy is amplified so is the enthalpy. We note that this is different from the free energy of mixing, where the mixing entropy decreases with the chain length but the enthalpy is not affected. In the case of $x = 2$, the last two terms will both decrease to zero and thus the formula of free energy returns to anisotropic small molecules in the Pople–Karasz model if further setting $D = 2$. In the other case, where the chain rigidity energy W_c and temperature satisfy the relation $W_c = k_B T \ln 2$, the sum of the last two terms will also be zero. This means the relative free energy of polymers can be the

same with small molecules at a certain temperature. Surely, it is not the monomers that are comparable with polymers but the small molecules that have the same magnitude of energy with the coarse-grained segments. The approximation $1 - 2/x \approx 1$ is always valid when $x \gg 2$, so the chain length should be a trivial parameter in the long-chain conditions. This is always the case in the properties of polymer phase transition. For example, with the increase of molecular weight, the properties of polymer liquid crystals change quickly when molecular weight is low but gradually become a constant value.⁴⁰ We will adopt this approximation in the following discussions.

RESULTS AND DISCUSSION

The thermodynamic equilibrium order parameters Φ and Θ at a certain temperature are calculated by searching the minimum of free energy. The free-energy landscape shows the minimized $\Delta G(\Phi, \Theta)$ satisfies the following equations

$$\begin{aligned} \frac{\partial}{\partial \Phi} \left(\frac{\Delta G}{Nk_B T} \right) = 0 & \Rightarrow \ln \frac{1+\Phi}{1-\Phi} \\ & = \Phi \frac{zW_{AB}}{k_B T} \left[\frac{1}{2} - \frac{(D-1)(1-\Theta^2)}{2D} v_1 \right] \end{aligned} \quad (10)$$

$$\begin{aligned} \frac{\partial}{\partial \Theta} \left(\frac{\Delta G}{Nk_B T} \right) = 0 & \Rightarrow \ln \frac{1+(D-1)\Theta}{1-\Theta} \\ & = \Theta \left\{ \frac{zW_{AB}}{k_B T} \left[\frac{(1+\Phi^2)}{2} v_1 + 2v_2 \right] - 2 \ln 2 \right\} \end{aligned} \quad (11)$$

In the above equations, we have set the ratios of energies

$$v_1 = z'W_{\alpha\alpha'}/zW_{AB} \quad v_2 = W_c/zW_{AB} \quad (12)$$

The two parameters are both measures of rigidity but have different physical meanings in nature. v_1 is the same as v_{PK} in the Pople–Karasz model that indicates the rigidity caused by intermolecular interactions, whereas v_2 results from the intramolecular interactions. In this way, the solutions of eqs 10 and 11 can be obtained as a function of $zW_{AB}/k_B T$ for a series of other parameters (v_1 , v_2 , and D). Pople and Karasz have calculated three typical forms of this function in small molecules under different values of v_{PK} .¹³ These have in common that, at a high temperature (small $zW_{AB}/k_B T$), the point $\Phi = \Theta = 0$, namely, the melt state, is always thermodynamically stable and at a low temperature (large $zW_{AB}/k_B T$), the stable state will approach the point $\Phi = \Theta = 1$, corresponding to the perfect crystal. The three forms are the following when considering the cooling process from disorder to order: (1) For flexible molecules, where the value of v_{PK} is small, the transition temperature (where order parameters start to deviate from the value of 0) of positional order parameter Φ is higher than that of orientational order parameter Θ , resulting in the appearance of plastic crystal phase. (2) For semiflexible molecules with an increased value of v_{PK} , when the two order parameters have the same transition temperature, no thermodynamically stable mesophases occur. (3) For rigid molecules that have a large value of v_{PK} , orientational ordering occurs first, thus a liquid crystal phase is predicted. By solving the polymer thermodynamic eqs 10 and 11, we obtain the numerical results of order parameters that satisfy the similar features mentioned above. It is indicated that the thermodynamic regularity of small molecules can be extended to

polymers. Actually, all three cases exist in real polymers. A high-pressure hexagonal phase (HHP) has been found in PE.^{41–43} The Raman spectra shows the chain conformation in HHP does not differ significantly from that in the melt,⁴¹ suggesting the nature of plastic crystal. Such a phase is not equal to that of a glass because it remains the feature of a crystal. The liquid crystals in the present model correspond to the thermotropic main chain liquid crystalline polymers. They are mostly copolymers of rigid and flexible components, first reported by Roviello and Sirigu.⁴⁴ Other crystalline polymers such as isotactic polypropylene should be classified into the semiflexible chain case since their conformational disordered crystal has been proved to be metastable.⁴⁵

To show the difference between polymers and small molecules, we make a comparison of the equilibrium order parameters, as illustrated in Figure 2. We choose $v_{PK} = 0.20$, 0.70, and 1.00, respectively, to represent the three modes in the Pople–Karasz model for the small molecule case. v_1 is set to be equal to v_{PK} , and v_2 is assigned to ensure the two transition temperatures are the same with as small molecules. In this way, the chain character of polymers in our modified twin-lattice model is highlighted. Figure 2a shows the comparison in flexible systems. The curves of Φ are complete coincidence regardless of the value of v_2 , suggesting the chain connectivity does not change the regularity of the positional order. However, orientational regularity is changed. At a temperature that is lower than the transition temperature ($zW_{AB}/k_B T > 10.22$), polymers tend to become a more orientational ordered state, compared with small molecules. It can be explained that, in this region of temperature, the enthalpy is the dominant contribution in free energy and polymers always possess more repulsion interactions. The deviation $\Delta\Theta = \Theta_p - \Theta_s$ increases with $zW_{AB}/k_B T$ until reaching a maximum of 0.116 at $zW_{AB}/k_B T = 11.68$ and finally becomes eliminated. When comparing semiflexible systems in Figure 2b, the curves of Φ and Θ are both coincidence, showing the chain connectivity is an insignificant factor in this case. It results from the fact that the equilibrium Θ instantly reaches the value of 1 (namely, complete orientation) just below the transition temperature, making the last two terms of eq 9 trivial. In rigid systems shown by Figure 2c, the situation becomes different. The positional order parameter Φ has an obvious dependence on v_2 , which means the coupling between Φ and Θ becomes significant. To make the two Φ curves coincident, the value of v_2 has to be fixed. In this case, we can discuss the results of liquid crystal states. The polymer liquid crystals are more disordered than small molecules in this case. The reason is probably that the additional entropy of polymers compensates the increased energy in the disordered state. Another phenomenon is that there is a maximum of orientational order parameter Θ_{max} in both polymeric and small molecular liquid crystals, which means the liquid crystal state cannot be completely ordered in orientation ($\Theta_{max} = 0.715$ in Figure 2c).

Evaluation of Thermodynamic Properties of Phase Transitions. Although we have found out the general features of phase transitions from the free energy, it is difficult to measure the variables directly from experiments. To further study the properties of phase transition from the equation of state, other thermodynamic functions that provide measurable quantities are needed. Among these functions, the pressure–volume isotherms are given by

$$P = P_1 + P_2 \quad (13)$$

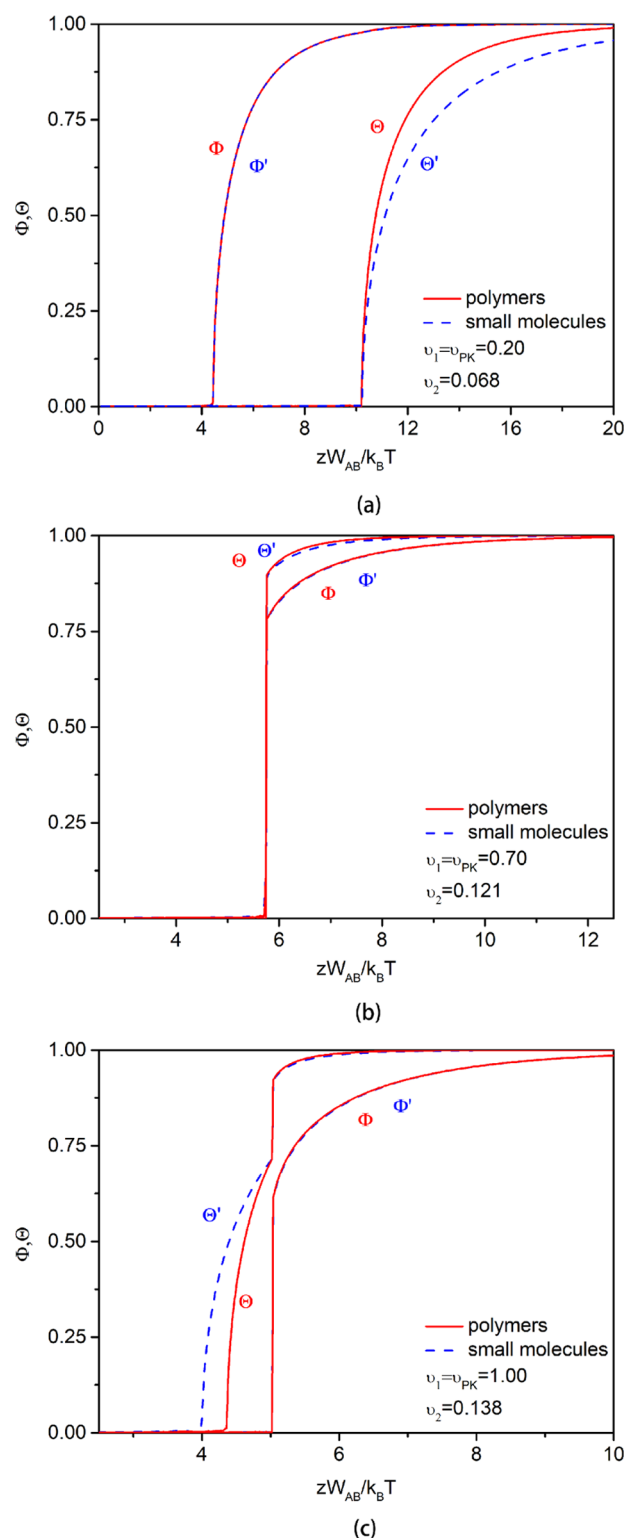


Figure 2. Comparison of equilibrium order parameters of polymers and small molecules as a function of $zW_{AB}/k_B T$ at $D = 2$. Φ and Θ are positional and orientational order parameters for polymers, Φ' and Θ' for small molecules. Φ and Φ' are almost coincident.

where P_1 is the pressure of the reference system, which has been calculated by Wentorf⁴⁶ on the basis of the free-volume theory and the 6–12 intermolecular energy law. We have extrapolated the data to relatively lower temperature. The other part P_2 is contributed from the disordering, which can be

derived from the thermodynamic correlation $P_2 = -(\partial \Delta G / \partial V)_{T,N}$. We follow the variation proposed by Pople and Karasz,¹³ supposing the parameters v_1 and v_2 are both independent of volume and the energy W_{AB} satisfies the following relation

$$W_{AB} = W_{AB}'(V_0/V)^4 \quad (14)$$

$$W_{AB}'/\varepsilon_0 = 0.977 \quad (15)$$

where V_0 is the standard volume if the segments are placed on a face-centered cubic lattice with a nearest neighboring distance of $2^{1/6}r_0$ and ε_0 is the energy minimum in the 6–12 intermolecular potential. So P_2 is given as follows

$$\frac{P_2 V_0}{N k_B T} = 4 \frac{V_0}{V} \frac{z W_{AB}}{k_B T} \left[\frac{(1 + \Phi)^2 + (1 - \Phi)^2}{4} \frac{(D - 1)(1 - \Theta^2)}{2D} v_1 + \frac{(D - 1)(1 - \Theta^2)}{D} v_2 + \frac{(1 + \Phi)(1 - \Phi)}{4} \right] \quad (16)$$

The order parameters in the above equation are the equilibrium values that satisfy eqs 10 and 11. When the reduced temperature $k_B T/\varepsilon_0$ is fixed, each reduced volume V/V_0 derives a value of $z W_{AB}/k_B T$ according to eqs 14 and 15, so the reduced pressure $P_2 V_0/N k_B T$ can be calculated from the equilibrium order parameters. By adding P_2 to P_1 , a complete isotherm is obtained. Typical isotherms are shown in Figure 3. The transition points of Φ and Θ result in the kinks in these curves. The total algebraic area from point A to C has been set to zero in an adjusted temperature, and thus A and C represent the two coexisting phases at $P = 0$. This is the so-called equal area principle. Phase A, which has higher density, is the more ordered phase, and phase C is the more disordered phase.

In Figure 3a where v_1 and v_2 are relatively small, either Φ or Θ transition point is included between A and C so two distinct temperatures will be found that match the equal area principle. At a lower temperature, the included point is Θ . Both phases A and C have positional ordering, but A is more ordered in orientation. At a higher temperature, the included point will be Φ . Although both A and C lost orientational ordering, A has more positional ordering than C. Phase transitions evaluated from the isotherms are consistent with the order parameter changes in Figure 2a, but more details are presented. Except for pressure and volume, the precise value of order parameters for each state is included so the entropies of phase transitions are accurately calculated. For phase A, it is at the point of $\Phi = 0.979$ and $\Theta = 0.816$, whereas for phase C, it is at $\Phi = 0.915$ and $\Theta = 0.002$. So the two phases are not completely ordered or disordered. This provides a suggestion that, if polymer chains are flexible enough, the process of conformational ordering will take place after translational ordering in crystallization. Thus, in this case, it will be possible to maintain the polymers in an intermediate state. When v_1 and v_2 are increased to critical values, the case changes to Figure 3b. Both Φ and Θ points are included between the coexisting phases A and C, so the phase transition appears at only one temperature. The most ordered phase A ($\Phi = 0.979$ and $\Theta = 0.965$) is directly converted into the most disordered phase C ($\Phi = 0.003$ and $\Theta = 0.002$). This mode of phase transition corresponds to the order parameters in Figure 2b, despite

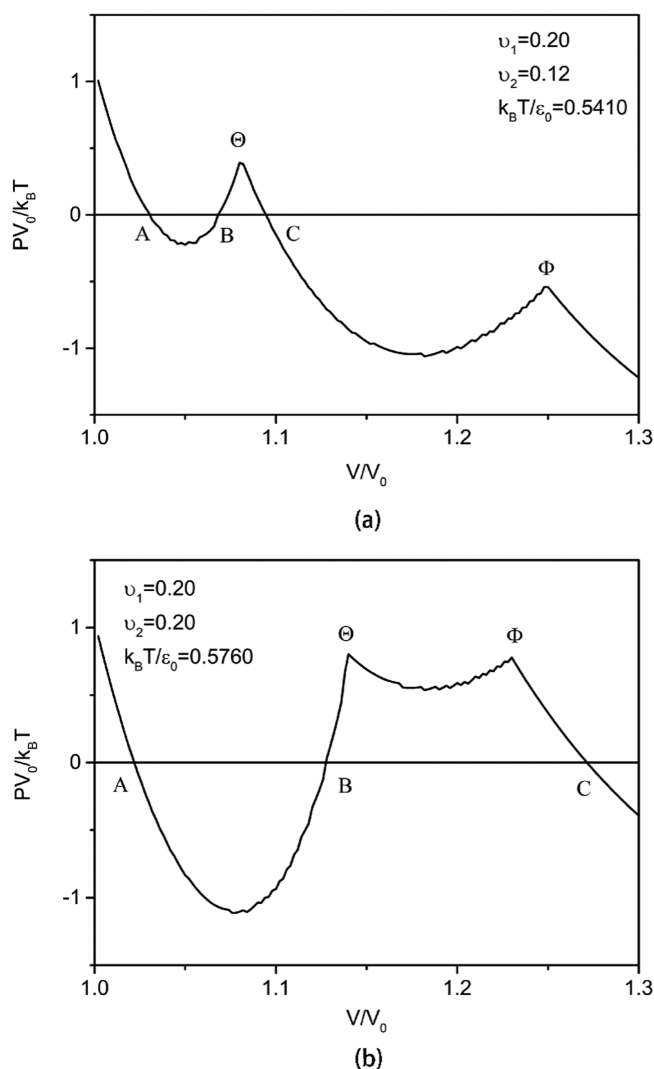


Figure 3. Typical isotherms at $D = 2$.

some deviations. What is illustrated is that when polymers are not completely flexible, there might be no thermodynamically stable mesophases, because the position and orientation will start to be ordered spontaneously in the condition of supercooling. The critical values of v_1 and v_2 are found to satisfy the following relation

$$v_1 + 1.88v_2 = 0.493 \quad (17)$$

at $D = 2$. Hence, we can define the parameter $v_a = v_1 + 1.88v_2$ to represent the apparent rigidity of polymers, which can be used to distinguish the two different behaviors of phase transition. At a higher value of v_1 (v_2), a smaller v_2 (v_1) is needed to reach the co-transition condition. However, this definition of v_a cannot be used in other cases. A universal definition of v_a is not available since eqs 10 and 11 are calculated numerically. However, the linear expression of the apparent rigidity is always valid so that v_1 and v_2 are truly the two aspects reflecting the rigidity of polymers. Besides, although liquid crystal is predicted, an investigation into it needs to modify the volumetric dependence of energy,¹⁹ which complicates the calculations. Although it is possible to bring new insights to the polymer system, we are not going to discuss this issue further in this paper and retain the primary expression.

In Figures 4–6, the reduced transition temperature $k_B T_{\text{trans}}/\epsilon_0$, relative volume change $\Delta V/V_0$, and entropy change $\Delta S/\epsilon_0$

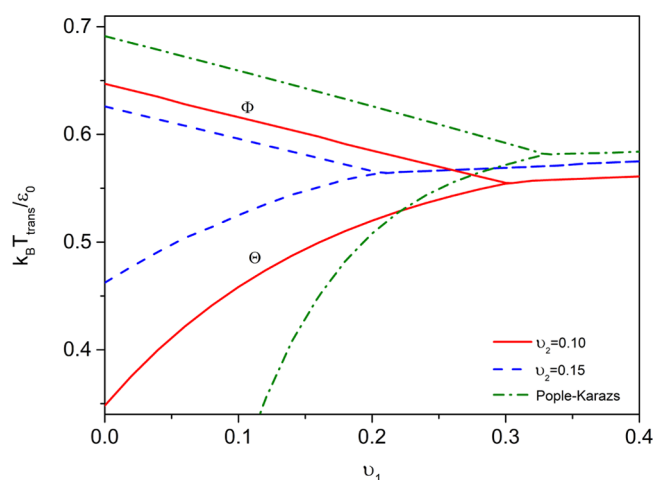


Figure 4. Reduced transition temperature $k_B T_{\text{trans}}/\epsilon_0$ as a function of v_1 for two values of v_2 at $D = 2$.

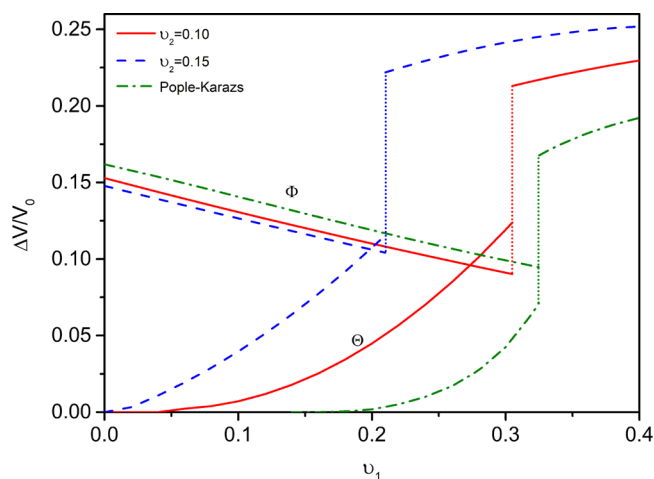


Figure 5. Relative volume change $\Delta V/V_0$ as a function of v_1 for two values of v_2 at $D = 2$.

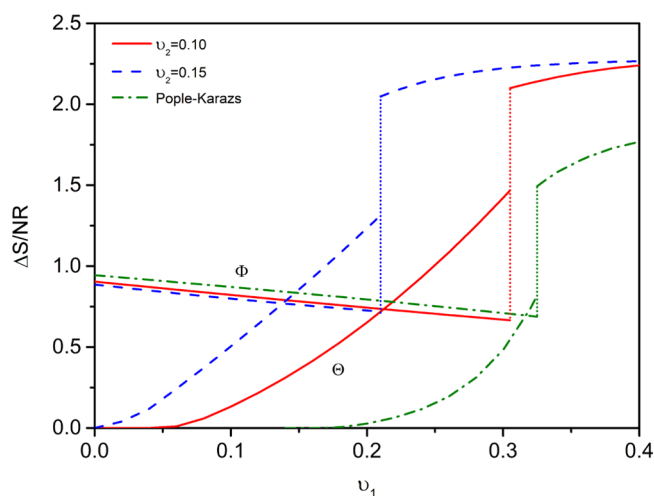


Figure 6. Entropy change $\Delta S/NR$ as a function of v_1 for two values of v_2 at $D = 2$.

NR, evaluated from Figure 3, are plotted as a function of v_1 for two values of v_2 (0.10 and 0.15) at $D = 2$. As has been mentioned, a critical value of v_a distinguishes two kinds of transitions and their difference is presented more clearly in these figures. In the figure of $k_B T_{\text{trans}}/\epsilon_0$ (Figure 4), the two transition temperatures gradually converge when v_1 or v_2 is increased from 0 to the critical value. It is to say that with more rigidity imparted to polymers, it becomes easier for orientational ordering but more difficult for positional ordering when cooled from the disordered phase, resulting in the decrease of Φ transition temperature and the increase of Θ transition temperature. Meanwhile, its dependence on D has been reported in Amzel and Becka's work.¹⁷ According to their results, the more orientations are permitted, the harder it is to arrange all bond vectors into the same direction. Hence, more rigidity is needed to obtain the co-transition behaviors. Above the critical value, the transition temperatures keep increasing but the increase is much more subdued. A comparison with the Pople–Karasz result¹³ shows the Θ transition temperature in polymers is less sensitive to v_1 . The case of $v_2 = 0$ will not match with that of small molecules as well, because of the existence of the conformational entropy in polymers even for a completely flexible chain.

Different from the continuous functions of temperature, the two modes of transitions lead to a discontinuity in relative volume changes, as shown in Figure 5. Below the critical values, the volume changes of Φ and Θ transitions evolve separately. The values of $\Delta V/V_0$ in Θ transition are enlarged with the increase of both v_1 and v_2 , indicating the difference of density between the perfect crystals and plastic crystals is larger in a more rigid system. In contrast, it is the opposite in the case of Φ transition. When converted from plastic crystal to the melt state, the volumes changes less for a rigid system. Comparing v_1 and v_2 , it is clear the melting process is less influenced by v_2 since ΔH_c is only a function of Θ . Beyond the critical values, $\Delta V/V_0$ changes into the summation of the Φ part and Θ part. As a result, although the total difference between the most ordered and the most disordered state remains continuous as a function of v_1 and v_2 , a jump can be found in the figure of each transition process. The increase in Θ part overwhelms the decrease in Φ part, so the overall $\Delta V/V_0$ keeps rising in this range of parameter values. The curve for $v_2 = 0.15$ is still in the upper bound of that for $v_2 = 0.10$. It corresponds to the fact that stiffer polymers always experience larger volume shrinkage in the whole process of crystallization. The difference between polymers and small molecules seems to be not so obvious in this figure so that the Pople–Karasz result is very close to that in the case of $v_2 = 0$. From the other point of view, a similar feature is calculated in $\Delta S/NR$ about its dependence on rigidity, which is illustrated in Figure 6. The reason is the volume represents the degree of freedom. Also, it should be said the mode of molecular motions is the same under different energetic parameters, whereas this is not the case for D effects; $\Delta S/NR$ has a significant dependence on D but $\Delta V/V_0$ does not. The above discussion enables us to make a comparison with experimental measurements.

Comparison with Experiments. To compare theoretical predictions with experimental results, we need to assign three values of v_1 , v_2 , and D to each compound, which is not directly supported by experiments or theories. Even if all parameters are accurately assigned, direct comparison is not easy to proceed with. Different from small molecules, the thermodynamic information of polymers is less complete, because the

chain-extended monocrystals at thermodynamic equilibrium are not easy to be obtained.²⁹ The measurement of thermodynamic properties is greatly influenced by dynamic factors. Although experimental estimation is available from semiempirical formulas such as the Hoffman–Weeks equation for equilibrium melting points,⁴⁷ there is still much suspicion in the thermodynamics of polymer crystallization. Many other factors break the regularities between intermolecular interactions and experimental observations. For example, because of the hydrogen-bond interaction, the melting points of polyamides are much higher than those of polyesters. The heats of fusion are supposed to be larger in polyamides as well, but the opposite result is observed in some cases.

To proceed with the thermodynamic comparison and minimize unfavorable factors, we choose *n*-paraffins for discussions. The reasons are as follows. They are oligomers of PE with the simplest hydrocarbon structures. It is clear the crystallization behaviors of *n*-paraffins and PE are very different, such as the chain folding behavior and degree of crystallinity. These differences, however, can be attributed to dynamics. In thermodynamics, they are less different. It has been published by Ungar³⁹ that the properties of phase transition from *n*-paraffins to polyethylene will satisfy a continuous function. The thermodynamics of PE can be directly extended from *n*-paraffins, because their free energies are composed of the same contributions (positional, orientational, and conformational). In addition, the thermodynamic properties of *n*-paraffins have been systematically investigated in numerous studies.^{48–52} Odd paraffins from C₉ to C₄₃ and even paraffins from C₂₂ to C₄₄ experience a first-order solid–solid transition (or rotator transition) from crystals into a so-called rotator phase, which was first discovered by Müller.⁵³ Such a rotator phase is essentially a plastic crystal. We have mentioned this kind of feature in the previous discussion of this paper, on the basis of the twin-lattice model description. Although the rotator phase only has rotational freedom along the long axis, similar to the two-dimensional plastic crystal of small molecules, it cannot be described in the Pople–Karasz model. The defective structures in the rotator phase not only bring intramolecular stress but also have the freedom to diffuse without energy barriers.⁵⁴ These features can be included in our present model. According to above reasons, *n*-paraffin is a suitable system for our comparison between calculations and experiments. Furthermore, we shall reconsider the influence of x and the other parameters are to be assigned on the basis of the existing data. Surely, other theories may give a better explanation for these observations.^{55,56} Our goal in this section is not to give a perfectly fitted result but to show the physics included in the present model.

Assignment of Parameters. Now that the parameter D in the twin-lattice model has been discussed by Amzel and Becka,¹⁷ we shall follow their strategy. In their discussions, the following relation proposed by Guthrie and McCullough⁵⁷ is verified

$$\Delta S_t = R \ln D \quad (18)$$

where ΔS_t is the entropy of solid–solid transition. When we apply eq 18 to polymeric solids, ΔS_t should be the entropy of each segment. In Table 1, the approximated D s of *n*-paraffins are listed and two kinds of segment structures are compared, on the basis of the experimental data summarized by Broadhurst⁴⁸ from C₁₁ to C₃₀. When the structure $-\text{CH}_2-$ is set as a segment of *n*-paraffins, the permitted number of

Table 1. Approximated D from Observed Entropies of *n*-Paraffins

carbon number	ΔS_t^a (cal/(K mol))	structure ^b	x^c	$\exp(\Delta S_t / xR)$	D^d
11	6.927	CH ₂	11	1.373	2
		CH ₂ CH ₂	6	1.788	
13	7.180		13	1.320	2
			7	1.676	
15	8.088		15	1.312	2
			8	1.663	
17	9.323		17	1.318	2
			9	1.684	
19	11.179		19	1.345	2
			10	1.755	
21	12.103		21	1.337	2
			11	1.740	
22	21.316		22	1.628	2
			11	2.652	
23	16.576		23	1.437	2
			12	2.004	
24	23.280		24	1.629	2
			12	2.655	
25	19.457		25	1.479	2
			13	2.124	
26	25.054		26	1.624	2
			13	2.638	
27	21.214		27	1.485	2
			14	2.144	
28	25.574		28	1.584	2
			14	2.508	
29	22.752		29	1.484	2
			15	2.145	
30	26.730		30	1.566	2
			15	2.452	

^aExperimental entropies of rotator transitions from ref 48. ^bStructure of segment. ^cEquivalent number of segments. ^dApproximated values.

orientations D will be less than 2, which means the rotational motion of each $-\text{CH}_2-$ group is hindered. When the structure of the segment is replaced by $-\text{CH}_2-\text{CH}_2-$, the value $D = 2$ is able to give a preferable fit with the experimental measurements. Thus, we assume that there will be two distinguishable rotational degrees of freedom in the motion of $-\text{CH}_2-\text{CH}_2-$. Further coarse graining will lead to larger values of D s, but more details will be lost, especially for finite-length chains. Therefore, the assumption of a two-carbon segment and $D = 2$ will be adopted. Besides, there is a distinction between the odd and even numbered paraffins, which results from different crystal structures. Due to different modes of packing in the end group layers, the crystals of odd paraffins are orthorhombic whereas even paraffins are triclinic or monoclinic.⁴⁸ We will adopt the data of odd paraffins in the following discussion because they have a better match with the above assumptions.

In the assignment of v_1 and v_2 , a special treatment is needed because of the nature of the *n*-paraffin rotator phases. The rotator phases have a unique symmetry, which is described by the terminology conformationally disordered crystal (Condis crystal).⁵⁸ In the present twin-lattice model, the percentage of defect structures in a plastic crystal phase is the same in any of the cases. However, according to the IR measurements and Raman analysis,^{59–61} the concentration of defect structures in the rotator phases of *n*-paraffins varies with the number of

carbon atoms. The primary twin-lattice expression cannot directly predict such a phenomenon; thus, we shall rewrite the free energy of *n*-paraffins as

$$\frac{\Delta G}{Nk_B T} = \left(\frac{\Delta H_p + \Delta H_l}{Nk_B T} - \frac{\Delta S_p + \Delta S_o}{Nk_B} \right) + \rho \left(\frac{\Delta H_c}{Nk_B T} - \frac{\Delta S_c}{Nk_B} \right) \quad (19)$$

where ρ is used to modify the contribution of the conformational part in free energy. Although it has been clear the defect concentrations increase nonlinearly with the carbon number,⁵⁹ we can still use a linear approximation for ρ to compare the deviation. According to the existing observations,⁵⁹ it is acceptable to say $\rho = 0$ in the C_{17} rotators because it only has few defect structures. The rotator phase of C_{33} is reported to possess about three gauche conformers per 100 carbon atoms.⁵⁸ In the twin-lattice model, however, the number of gauche conformers is supposed to be 47 per 100 carbons. This comparison allows us to estimate $\rho = 0.064$ for C_{33} . By fitting with the experimental value of T_t/T_m the ratio of rotator transition temperature and melting temperature of C_{17} and C_{33} , we have $\nu_1 = 0.30$ and $\nu_2 = 0.22$ for the best fit. The values of ρ in other *n*-paraffins between C_{17} and C_{33} are distributed linearly between 0 and 0.064. Extrapolation of the linear relation is applied for *n*-paraffins beyond C_{33} . These estimations are listed in Table 2.

Table 2. Experimental and Calculated Values of Rotator and Melting Temperatures

carbon number	experimental values ^a			ρ^b	$T'_t/T'_m{}^c$
	T_t (K)	T_m (K)	T_t/T_m		
17	283.7	295.1	0.9614	0	0.9621
19	295.2	305.2	0.9672	0.008	0.9655
21	305.7	313.4	0.9754	0.016	0.9688
23	313.7	320.7	0.9782	0.024	0.9722
25	320.2	326.7	0.9801	0.032	0.9755
27	326.2	332.0	0.9825	0.040	0.9788
29	331.4	336.6	0.9846	0.048	0.9821
31	336.2	340.9	0.9862	0.056	0.9854
33	340.6	344.3	0.9893	0.064	0.9887
35	345.1	347.7	0.9925	0.072	0.9920
37	348.7	350.6	0.9946	0.080	0.9952
39	352.3	353.5	0.9966	0.088	0.9981
41	355.5	356.1	0.9983	0.096	1
43	358.4	358.5	0.9997	0.104	1
45			1	0.112	1
47			1	0.120	1
49			1	0.128	1
51			1	0.136	1

^aExperimental values of rotator and melting temperatures from ref 48.

^bLinear estimation based on C_{17} and C_{33} . ^cCalculated values of rotator and melting temperatures with the parameters $\nu_1 = 0.30$, $\nu_2 = 0.22$, and $D = 2$.

Direct Comparison with Experiments. With the parameters properly assigned, it is possible to compare the predicted values directly with experimental observations. As shown in Figure 7, the theoretical and experimental values of T_t/T_m are plotted as a function of carbon numbers from 17 to 51. See also Table 2. In experimental observation, the rotator

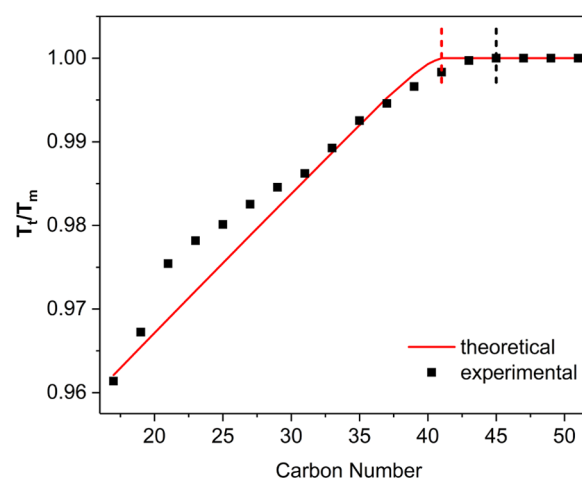


Figure 7. Comparison of the theoretical with the experimental rotator transition/melting temperature ratio T_t/T_m as a function of the carbon number. Experimental data is from ref 48. See also Table 2.

phase of *n*-paraffins only occurs at a temperature slightly below the melting point so the measured T_t/T_m 's are located in a narrow interval from 0.96 to 1.00. When $C < 45$, the value of T_t/T_m increases with carbon numbers. When $C \geq 45$, the rotator transitions disappear and T_t/T_m becomes a constant at 1. The present model reproduces this feature, when we increase the contribution of the conformational part in free energy or the values of ρ with carbon numbers. In our prediction, the rotator transitions will be obtained when the segment number is set from 9 to 20, corresponding to C_{17} to C_{39} . The upper boundary is very close to the experimental observation. In spite of the crude approximation, the experimental points agree well with the calculated values, especially for C_{29} to C_{39} , which means the assumption of the linear increase of ρ is reasonable in this region. The result also suggests the increased defect concentration may be a possible driving force for the disappearance of the *n*-paraffin rotator phases. As the *n*-paraffin chains get longer, it becomes easier to form defect structures after rotator transition. As a result, the transitions of orientational order parameter in *n*-paraffins will occur at a relatively higher temperature. When the melting and rotating processes become comparative, the rotator phase will no longer exist. Surely, there is an apparent discrepancy for C_{21} to C_{29} , whose predicted values of T_t/T_m are lower than the observed ones. Such a discrepancy comes from the complex polymorphs of *n*-paraffin rotators. Some updated researches have revealed there are totally five distinct rotator phases, which are denominated as R_1 to R_5 , respectively.⁴⁹ More kinds of phase transitions have been detected. For example, C_{23} transfers from crystal to R_5 at 311 K, and then changes into R_1 at 314.3 K.⁶² These details are beyond our ability while discussing the present model. Generally speaking, we can still say the present model well explains the disappearance of rotator phases in *n*-paraffins.

To verify the assumption of eq 18, which has been used to estimate the value of D , the predicted and observed entropies of rotator transition $\Delta S_t/R$ are replotted as a function of the carbon number, shown in Figure 8. Although we cannot predict the entropy decrease from C_{29} to C_{31} , the overall agreement is good, indicating the assumption of a two-carbon segment and $D = 2$ works very well. The result further verifies that eq 18 is still reliable in estimating the independent

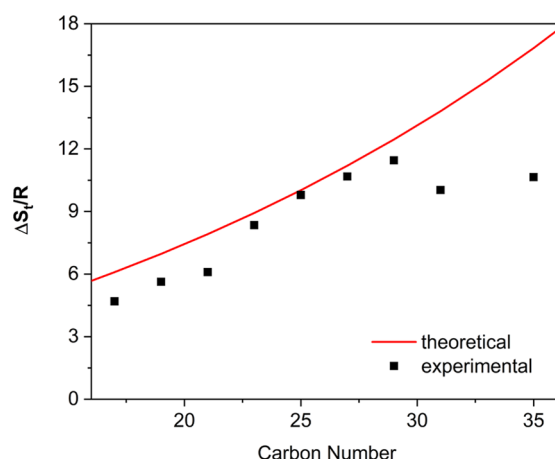


Figure 8. Comparison of theoretical with experimental entropies of rotator transition $\Delta S_t/R$ as a function of the carbon number. For experimental points, see also Table 1.

rotational freedom of polymeric molecules. The increased entropy in a longer molecule is not only a result of the additional carbon atoms but also the higher concentration of defects in the rotator phase. What is out of our expectation is the calculated entropies of rotator transition are higher than the observed ones. This case is supposed to be the opposite because we have modified the conformational entropies. The reason may be the overestimation of the translational and orientational entropies, considering the unique symmetry of the Condis crystals.

Finally, we make a comparison of the volume changes in phase transitions, shown in Table 3. The available experimental

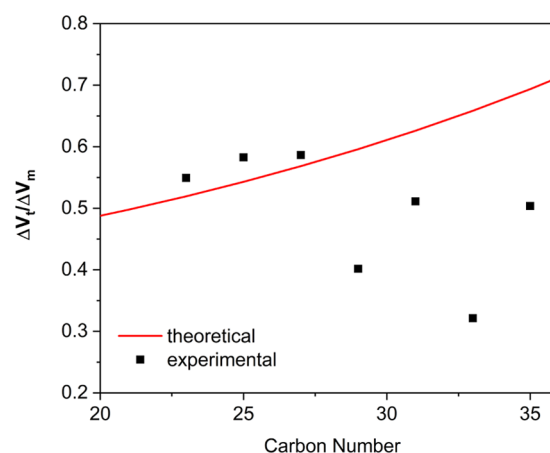


Figure 9. Comparison of theoretical with experimental rotator transition/melting volume change ratio $\Delta V_t/\Delta V_m$ as a function of carbon number. For experimental points, see also Table 3.

of the odd-numbered *n*-paraffins, the discrepancy in Figure 9 might be another aspect of the even–odd paraffin differences.

Now that the twin-lattice model has well explained the phase transition behaviors of *n*-paraffins, we can expect it to apply to the crystallization of other polymers or the dynamics. The Flory–Huggins free-energy functional for polymer blends has been used to study the phase separation dynamics, known as the time-dependent Ginzburg–Landau equation.⁶⁶ The extension to dynamics of this model can be performed in a similar way, because it has provided an expression of the free-energy functional for crystallization process and the parameters in the dynamic equations can translate into the quantities in the twin-lattice model. In addition, some observations shall be understood by solving the dynamic equation of the two nonconserved order parameters.⁶⁷ Stepanow⁶⁸ proposed an idea that a finite lamellar thickness of a polymer crystal is a result of the competition between the “formation of stems” and the “relaxation back to random coil shape”, which is analogous to the competition between positional and orientational order parameter in this paper. Although there are other factors to consider, we are holding the expectation for solving the problems of dynamics.

CONCLUSIONS

This paper depicts a new understanding of polymer crystallization by the modified twin-lattice model. The thermodynamics of order and disorder in polymers is presented in an intuitive way. Without complicated calculations, the free energy of polymers is directly obtained by introducing the conformational energy and entropy on the basis of small molecules. Then, we calculate the equilibrium state by order parameters. The thermodynamics of polymers differs from that of small molecules because of the intramolecular defect structures, which is the most specific feature of polymers. The two energetic parameters v_1 and v_2 defined in the free-energy formula present the two aspects of rigidity, including the lattice energy caused by rotational motions and conformational energy by the appearance of nonlinear conformers. Together, they decide the apparent rigidity of polymers, which distinguishes the different processes of crystallization. All of these features become countable in the twin-lattice description. The calculation shows the inert rigidity has a more significant impact on the orientation-related

Table 3. Theoretical and Experimental Values of ΔV_t and ΔV_m

carbon number	theoretical ^a			experimental		
	$\Delta V_t/V_0$	$\Delta V_m/V_0$	$\Delta V_t/\Delta V_m$	ΔV_t (cm ³ /g)	ΔV_m (cm ³ /g)	$\Delta V_t/\Delta V_m$
23	0.050	0.098	0.519	0.067	0.122	0.549
25	0.054	0.096	0.543	0.074	0.127	0.583
27	0.056	0.098	0.568	0.078	0.133	0.586
29	0.058	0.096	0.596	0.053	0.132	0.402
31	0.060	0.098	0.626	0.069	0.135	0.511
33	0.064	0.098	0.658	0.044	0.137	0.321
35	0.068	0.098	0.694	0.069	0.137	0.504

^aExperimental data from refs 63 and 64.

data is from Templin⁶³ and Seyer⁶⁴ for the even numbered *n*-paraffins from C₂₄ to C₃₆. The ratios of volume changes in the rotating and melting transition processes $\Delta V_t/\Delta V_m$ are chosen, plotted as a function of the chain length in Figure 9. The experimental observations do not show a clear relation between the two variables. There is a slight increase before C₂₉ but quickly changes into a zigzag style. The reason might be the complex solid–solid transition,^{62,65} as has been discussed in the previous paragraph. However, our calculation predicts a monotonically increased relation. It is a result of the increased ΔV_t because ΔV_m is much less sensitive to the concentration of defects. In spite of the discrepancy, the observed ΔV_m in experiment, indeed, has only changed slightly. Since the parameters we use match better with those

processes like the solid–solid transition from crystal to plastic crystal. In particular, the disappearance of rotator phases in *n*-paraffins is well explained by our twin-lattice model method, proving its potential applications for understanding other phenomena including dynamics in polymer crystallization.

APPENDIX

ΔS_c is derived in the following process by referring the Flory–Huggins lattice theory for polymer solutions.

1. In the hypothetical two-set lattice for accommodating N segments, it is supposed j polymer chains have been arranged, among which $jx(1 + \Phi)/2$ segments are in α site and the rest $jx(1 - \Phi)/2$ segments are in β site.
2. It is further supposed the newly added $j + 1$ th chain does not change the order parameters of the system, so in this chain $x(1 + \Phi)/2$ segments shall be arranged to α site and the rest $x(1 - \Phi)/2$ segments shall be arranged to β site.
3. Each arranged segment will increase the possibility that a site is occupied. So the possibility that the $j + 1$ th chain can be fully accommodated is as follows

$$p_{j+1} = \frac{1}{N^{x-1}} \frac{\left(N - \frac{jx(1+\Phi)}{2}\right)!}{\left(N - \frac{(j+1)x(1+\Phi)}{2}\right)!} \frac{\left(N - \frac{jx(1-\Phi)}{2}\right)!}{\left(N - \frac{(j+1)x(1-\Phi)}{2}\right)!} \quad (20)$$

4. After arranging the first segment, the second segment should be placed in the front or backward place of the first bond. If the second bond is in the same orientation with the first bond, the location of the third segment is located because the chain should remain in the extended conformation. If the second bond is in a different orientation, again the third segment can choose the front or backward place of the second bond. Each time there is a pair of neighboring bonds in different orientations, the next segment will have to choose one of two orientations and thus contribute a new conformation. We regard the segment connecting such pair of bonds as the “defect”. On an average, the number of defects in the $j + 1$ th chain is $(x - 2)(D - 1)(1 - \Theta^2)/D$, where the minuend 2 means the two terminal segments and they should not be included in the defects. The total number of conformations in the chain is

$$\omega_{j+1} = \frac{2 \times 2^{(x-2)(D-1)(1-\Theta^2)/D}}{2!2!} \quad (21)$$

where one of the two 2s in the denominator represents the equivalence of α and β sites and the other represents the equivalence of the “head” and “tail” segments.

5. By summing the whole chains, we obtain the absolutely conformational entropy

$$\begin{aligned} \frac{S_c}{Nk_B} &= \ln \left[\frac{1}{n_p!} \prod_{j=0}^{n_p-1} p_{j+1} \omega_{j+1} \right] \\ &= \left(1 - \frac{2}{x}\right) \frac{(D-1)(1-\Theta^2)}{D} \ln 2 \\ &\quad - \frac{1}{2} [(1 + \Phi) \ln(1 + \Phi) + (1 - \Phi) \ln(1 - \Phi)] + K \end{aligned} \quad (22)$$

where K is a constant unrelated with the order parameters, which should be included in the reference system, and the second part can be classified into ΔS_p . So we have the final eq 4.

AUTHOR INFORMATION

Corresponding Authors

*E-mail: pingtang@fudan.edu.cn (P.T.).

*E-mail: yuliangyang@fudan.edu.cn (Y.Y.).

ORCID

Ping Tang: 0000-0003-0253-1836

Notes

The authors declare no competing financial interest.

ACKNOWLEDGMENTS

We thank financial supports from the National Natural Science Foundation of China (Grant Nos. 21534002, 21574027, and 21774027).

REFERENCES

- (1) Cheng, S. Z. D.; Keller, A. The role of metastable states in polymer phase transitions: Concepts, principles, and experimental observations. *Annu. Rev. Mater. Sci.* **1998**, *28*, 533–562.
- (2) Wunderlich, B. Thermodynamic description of condensed phases. *J. Therm. Anal. Calorim.* **2010**, *102*, 413–424.
- (3) Landau, L. D.; Lifshitz, E. M.; Pitaevskii, L. *Statistical Physics, Part I*; Pergamon: Oxford, 1980.
- (4) Lennard-Jones, J. E.; Devonshire, A. F. Critical and co-operative phenomena III A theory of melting and the structure of liquids. *Proc. R. Soc. A* **1939**, *169*, 317–338.
- (5) Kobayashi, R. Modeling and numerical simulations of dendritic crystal growth. *Phys. D* **1993**, *63*, 410–423.
- (6) Caginalp, G.; Fife, P. Phase-field methods for interfacial boundaries. *Phys. Rev. B* **1986**, *33*, 7792.
- (7) Xu, H.; Matkar, R.; Kyu, T. Phase-field modeling on morphological landscape of isotactic polystyrene single crystals. *Phys. Rev. E* **2005**, *72*, No. 011804.
- (8) Oxtoby, D. W. New perspectives on freezing and melting. *Nature* **1990**, *347*, 725–730.
- (9) Monson, P. A.; Kofke, D. A. In *Solid–Fluid Equilibrium: Insights from Simple Molecular Models*; Prigogine, I., Rice, S. A., Eds.; Advances in Chemical Physics; John Wiley & Sons Inc.: New York, 2000; Vol. 115, pp 113–179.
- (10) Ram, J. Equilibrium theory of molecular fluids: Structure and freezing transitions. *Phys. Rep.* **2014**, *538*, 121–185.
- (11) Maier, W.; Saupe, A. Eine einfache molekular-statistische Theorie der nematischen kristallin-flüssigen Phase. Teil II. *Z. Naturforsch. A* **1959**, *14*, 882–889.
- (12) Prost, J. *The Physics of Liquid Crystals*; Oxford University Press, 1995; Vol. 83.
- (13) Pople, J. A.; Karasz, F. E. Theory of fusion of molecular crystals I. The effects of hindered rotation. *J. Phys. Chem. Solids* **1961**, *18*, 28–39.

- (14) Karasz, F. E.; Pople, J. A. A theory of fusion of molecular crystals II: Phase diagrams and relations with solid state transitions. *J. Phys. Chem. Solids* **1961**, *20*, 294–306.
- (15) Würflinger, A. Differential thermal analysis under high pressure IV: Low-temperature DTA of solid-solid and solid-liquid transitions of several hydrocarbons up to 3 kbar. *Ber. Bunsen-Ges. Phys. Chem.* **1975**, *79*, 1195–1201.
- (16) Smith, G. W. Proton Magnetic Resonance Studies of Solid Tetramethyls of Silicon, Germanium, Tin, and Lead. *J. Chem. Phys.* **1965**, *42*, 4229–4243.
- (17) Amzel, L.; Becka, L. A model for the evaluation of thermodynamic properties for the solid-solid and melting transitions of molecular crystals. *J. Phys. Chem. Solids* **1969**, *30*, 521–538.
- (18) Chandrasekhar, S.; Shashidhar, R.; Tara, N. Theory of melting of molecular crystals: the liquid crystalline phase. *Mol. Cryst. Liq. Cryst.* **1970**, *10*, 337–358.
- (19) Chandrasekhar, S.; Shashidhar, R.; Tara, N. Theory of melting of molecular crystals II: Solid-solid and melting transitions. *Mol. Cryst. Liq. Cryst.* **1971**, *12*, 245–250.
- (20) Chandrasekhar, S.; Shashidhar, R. Theory of melting of molecular crystals III: the effect of short range orientational order on liquid crystalline transitions. *Mol. Cryst. Liq. Cryst.* **1972**, *16*, 21–32.
- (21) Özgan, Ş.; Keskin, M. A theory of melting of molecular crystals. 2. Phase diagrams and relations with solid state transitions. *Mol. Cryst. Liq. Cryst. Sci. Technol., Sect. A* **1995**, *270*, 135–146.
- (22) Özgan, Ş.; Keskin, M. A theory of melting of molecular crystals. 3. The liquid crystalline phase. *Mol. Cryst. Liq. Cryst. Sci. Technol., Sect. A* **1995**, *270*, 147–157.
- (23) Keskin, M.; Özgan, Ş. A theory of melting of molecular crystals. 1. Theory and evaluation of the thermodynamic properties of melting. *Mol. Cryst. Liq. Cryst. Sci. Technol., Sect. A* **1995**, *269*, 149–163.
- (24) Özgan, Ş.; Keskin, M. A theory of melting of molecular crystals. 4. The complete picture of transition temperatures. *Mol. Cryst. Liq. Cryst. Sci. Technol., Sect. A* **1996**, *287*, 265–268.
- (25) Özgan, Ş.; Yazıcı, M.; Keskin, M. Dynamic behaviour of the modified Pople-Karasz model. *Phys. A* **2003**, *317*, 354–370.
- (26) Hu, W. B.; Frenkel, D. Polymer Crystallization Driven by Anisotropic Interactions. In *Interphases and Mesophases in Polymer Crystallization III*; Allegra, G., Ed.; Springer-Verlag: Berlin, 2005; Vol. 191, pp 1–35.
- (27) Kaji, K.; Nishida, K.; Kanaya, T.; Matsuba, G.; Konishi, T.; Imai, M. Spinodal Crystallization of Polymers: Crystallization from the Unstable Melt. In *Interphases and Mesophases in Polymer Crystallization III*; Allegra, G., Ed.; Springer-Verlag: Berlin, 2005; Vol. 191, pp 187–240.
- (28) Cui, K.; Ma, Z.; Tian, N.; Su, F.; Liu, D.; Li, L. Multiscale and multistep ordering of flow-induced nucleation of polymers. *Chem. Rev.* **2018**, *118*, 1840–1886.
- (29) Zhang, M. C.; Guo, B.-H.; Xu, J. A review on polymer crystallization theories. *Crystals* **2017**, *7*, 4.
- (30) Li, Z. L.; Zhou, D. S.; Hu, W. B. Recent progress on flash DSC study of polymer crystallization and melting. *Acta Polym. Sin.* **2016**, 1179–1197.
- (31) Zha, L. Y.; Hu, W. B. Molecular simulations of confined crystallization in the microdomains of diblock copolymers. *Prog. Polym. Sci.* **2016**, *54–55*, 232–258.
- (32) Flory, P. J. *Principles of Polymer Chemistry*; Cornell University Press, 1953.
- (33) Huggins, M. L. Solutions of long chain compounds. *J. Chem. Phys.* **1941**, *9*, 440–440.
- (34) Brock, J. D. Bond-Orientational Order. In *Bond-Orientational Order in Condensed Matter Systems*; Strandburg, K. J., Ed.; Partially Ordered Systems; Springer, 1992; pp 1–31.
- (35) Bragg, W. L.; Williams, E. J. The effect of thermal agitation on atomic arrangement in alloys. *Proc. R. Soc. A* **1934**, *145*, 699–730.
- (36) McCullough, R. An energetics approach to the analysis of molecular motions in polymeric solids. *J. Macromol. Sci., Part B: Phys.* **1974**, *9*, 97–139.
- (37) Kratky, O.; Porod, G. Röntgenuntersuchung gelöster fadenmoleküle. *Recl. Trav. Chim. Pays-Bas* **1949**, *68*, 1106–1122.
- (38) Saitô, N.; Takahashi, K.; Yunoki, Y. The statistical mechanical theory of stiff chains. *J. Phys. Soc. Jpn.* **1967**, *22*, 219–226.
- (39) Ungar, G. From plastic-crystal paraffins to liquid-crystal polyethylene: continuity of the mesophase in hydrocarbons. *Macromolecules* **1986**, *19*, 1317–1324.
- (40) Blumstein, R. B.; Stickles, E.; Gauthier, M.; Blumstein, A.; Volino, F. Influence of molecular weight on phase transitions and alignment of a thermotropic nematic polyester. *Macromolecules* **1984**, *17*, 177–183.
- (41) Tanaka, H.; Takemura, T. Studies on the high-pressure phases of polyethylene and poly(tetrafluoroethylene) by Raman spectroscopy. *Polym. J.* **1980**, *12*, 355.
- (42) Asahi, T. The hexagonal phase and melt of low-molecular-weight polyethylene. *J. Polym. Sci., Polym. Phys. Ed.* **1984**, *22*, 175–182.
- (43) Priest, R. G. Calculation of the high-pressure phase diagram of polyethylene. *Macromolecules* **1985**, *18*, 1504–1508.
- (44) Roviello, A.; Sirigu, A. Mesophasic structures in polymers. A preliminary account on the mesophases of some poly-alkanoates of p,p'-di-hydroxy- α,α' -di-methyl benzalazine. *J. Polym. Sci., Polym. Lett. Ed.* **1975**, *13*, 455–463.
- (45) Cocca, M.; Androsch, R.; Righetti, M. C.; Malinconico, M.; Di Lorenzo, M. L. Conformationally disordered crystals and their influence on material properties: The cases of isotactic polypropylene, isotactic poly(1-butene), and poly(L-lactic acid). *J. Mol. Struct.* **2014**, *1078*, 114–132.
- (46) Wentorf, R., Jr.; Buehler, R.; Hirschfelder, J.; Curtiss, C. Lennard-Jones and Devonshire Equation of State of Compressed Gases and Liquids. *J. Chem. Phys.* **1950**, *18*, 1484–1500.
- (47) Hoffman, J. D.; Weeks, J. J. Melting process and the equilibrium melting temperature of polychlorotrifluoroethylene. *J. Res. Natl. Bur. Stand., Sect. A* **1962**, *66A*, 13–28.
- (48) Broadhurst, M. G. An analysis of the solid phase behavior of the normal paraffins. *J. Res. Natl. Bur. Stand., Sect. A* **1962**, *66A*, 241–249.
- (49) Mukherjee, P. K. Phase transitions among the rotator phases of the normal alkanes: A review. *Phys. Rep.* **2015**, *588*, 1–54.
- (50) Dirand, M.; Bouroukba, M.; Chevallier, V.; Petitjean, D.; Behar, E.; Ruffier-Meray, V. Normal alkanes, multialkane synthetic model mixtures, and real petroleum waxes: crystallographic structures, thermodynamic properties, and crystallization. *J. Chem. Eng. Data* **2002**, *47*, 115–143.
- (51) Roblès, L.; Mondieig, D.; Haget, Y.; Cuevas-Diarte, M. A. Review on the energetic and crystallographic behaviour of n-alkanes. II. Series from C22H46 to C27H56. *J. Chim. Phys. Phys.-Chim. Biol.* **1998**, *95*, 92–111.
- (52) Espeau, P.; Roblès, L.; Mondieig, D.; Haget, Y.; Cuevas-Diarte, M. A.; Oonk, H. A. J. Review on the energetic and crystallographic behaviour of n-alkanes. 1. Series form C8H18 up to C21H44. *J. Chim. Phys. Phys.-Chim. Biol.* **1996**, *93*, 1217–1238.
- (53) Müller, A. The crystal structure of the normal paraffins at temperatures ranging from that of liquid air to the melting points. *Proc. R. Soc. A* **1930**, *127*, 417–430.
- (54) Mansfield, M.; Boyd, R. H. Molecular motions, the α relaxation, and chain transport in polyethylene crystals. *J. Polym. Sci., Polym. Phys. Ed.* **1978**, *16*, 1227–1252.
- (55) Mukherjee, P. K. Simple Landau model of the R-IV-R-III-R-V rotator phases of alkanes. *J. Chem. Phys.* **2008**, *129*, No. 021101.
- (56) Cantor, R. S.; Dill, K. A. Statistical thermodynamic theory for the melting of n-alkanes from their rotator phases. *Macromolecules* **1985**, *18*, 1875–1882.
- (57) Guthrie, G.; McCullough, J. Some observations on phase transformations in molecular crystals. *J. Phys. Chem. Solids* **1961**, *18*, 53–61.
- (58) Wunderlich, B.; Grebowicz, J. Thermotropic mesophases and mesophase transitions of linear, flexible macromolecules. *Adv. Polym. Sci.* **1984**, *60–61*, 1–59.

- (59) Maroncelli, M.; Strauss, H. L.; Snyder, R. G. The distribution of conformational disorder in the high-temperature phases of the crystalline n-alkanes. *J. Chem. Phys.* **1985**, *82*, 2811–2824.
- (60) Maroncelli, M.; Qi, S. P.; Strauss, H. L.; Snyder, R. G. Nonplanar conformers and the phase behavior of solid n-alkanes. *J. Am. Chem. Soc.* **1982**, *104*, 6237–6247.
- (61) Kotula, A. P.; Walker, A. R. H.; Migler, K. B. Raman analysis of bond conformations in the rotator state and premelting of normal alkanes. *Soft Matter* **2016**, *12*, 5002–5010.
- (62) Sirota, E.; King, H., Jr.; Singer, D.; Shao, H. H. Rotator phases of the normal alkanes: An X-ray scattering study. *J. Chem. Phys.* **1993**, *98*, 5809–5824.
- (63) Templin, P. R. Coefficient of volume expansion for petroleum waxes and pure n-paraffins. *Ind. Eng. Chem.* **1956**, *48*, 154–161.
- (64) Seyer, W. F.; Patterson, R. F.; Keays, J. L. The density and transition points of the n-paraffin hydrocarbons. *J. Am. Chem. Soc.* **1944**, *66*, 179–182.
- (65) Sirota, E.; Singer, D. Phase transitions among the rotator phases of the normal alkanes. *J. Chem. Phys.* **1994**, *101*, 10873–10882.
- (66) Fialkowski, M.; Holyst, R. Dynamics of phase separation in polymer blends revisited: Morphology, spinodal, noise, and nucleation. *Macromol. Theory Simul.* **2008**, *17*, 263–273.
- (67) Kyu, T.; Chiu, H.-W.; Guenther, A.; Okabe, Y.; Saito, H.; Inoue, T. Rhythmic growth of target and spiral spherulites of crystalline polymer blends. *Phys. Rev. Lett.* **1999**, *83*, 2749–2752.
- (68) Stepanow, S. Kinetic mechanism of chain folding in polymer crystallization. *Phys. Rev. E* **2014**, *90*, No. 032601.